Dynamic Control System Design for Autonomous Car

Shoaib Azam[a], Farzeen Munir[b] and Moongu Jeon[c]
*School of Electrical Engineering and Computer Science, Gwangju Institute of Science and Technology,
Gwangju, South Korea*

Keywords: Longitudinal Control, Lateral Control, Model Predictive Control, Pure Pursuit.

Abstract: The autonomous vehicle requires higher standards of safety to maneuver in a complex environment. We focus on control of the self-driving vehicle that includes the longitudinal and lateral dynamics of the vehicle. In this work, we have developed a customized controller for our KIA Soul self-driving car. The customized controller implements the PID control for throttle, brake, and steering so that the vehicle follows the desired velocity profile, which enables a comfortable and safe ride. Besides, we have also catered the lateral dynamic model with two approaches: pure pursuit and model predictive control. An extensive analysis is performed between pure pursuit and its adversary model predictive control for the efficacy of the lateral model.

1 INTRODUCTION

The 4^{th} industrial revolution brings about the cyber-physical system into the 21^{st} century. Among the fascinating technologies, the autonomous vehicle has captured the center stage, which promises to bring about the potential metamorphic impact on automotive transportation, environment, and social benefit (Lee et al., 2018). The progress of an autonomous vehicle is evaluated on the level of autonomy. The Society of Automation Engineering (SAE) has distinguished six levels of autonomy (SAE,). Level 0 is manual control, and level 5 is the fully autonomous mode, where the car is self-aware of the environment and intelligent enough to make sensible decisions. The increase in the level of automation is directly proportional to the ability of the autonomous vehicle to demonstrate precise control in the complex urban scenario.

The successful automation of the vehicle demands a perfect synchronization of environmental mapping for perception to the execution of the control commands(Thomanek and Dickmanns, 1995). Humans conscious do this job effortlessly, but developing this behavior in the vehicle requires additional sensors like camera, Lidar, GNSS, IMU, and Radar to be installed. In addition to the sensors, advanced machine learning algorithms are implemented that solve the problem of localization, object detection, object recognition, motion planning, path planning, and automatic control (Ziegler et al., 2014)(apo,) (Munir et al., 2018) (Acosta et al., 2017).

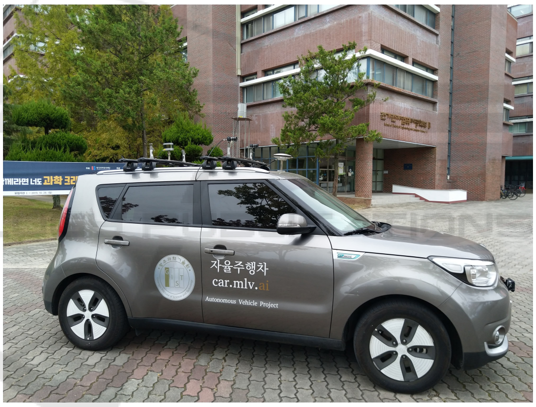

Figure 1: Our Self-Driving Car Equipped with State-of-the-Art Sensors That Includes Lidar, IMU, GNSS, Camera and Radar.

The problem of automatic control, focuses on manipulating the actuators such that the vehicle navigates with the desired speed and follows the path defined by the planning module (Rupp and Stolz, 2017). Therefore, the accuracy of automatic control is vital to safety and substantial to the autonomous vehicle. The automatic control of the autonomous vehicle consists of lateral control and longitudinal control(Jiang and Astolfi, 2018). The lateral control commands the steering angle of the vehicle that controls the head-

[a] https://orcid.org/0000-0003-3521-5098
[b] https://orcid.org/0000-0002-6760-4373
[c] https://orcid.org/0000-0002-2775-7789

Azam, S., Munir, F. and Jeon, M.
Dynamic Control System Design for Autonomous Car.
DOI: 10.5220/0009392904560463
In *Proceedings of the 6th International Conference on Vehicle Technology and Intelligent Transport Systems (VEHITS 2020)*, pages 456-463
ISBN: 978-989-758-419-0

ing direction, whereas the longitudinal control is concerned with regulating the speed of the vehicle, which is represented by a first-order system. The lateral control dynamics are modeled by the kinematic bicycle model or dynamic bicycle model(Jun et al., 2018).

In literature, the researchers have utilize the classical controller such as Proportional-Integral-Derivative (PID) control (Pérez et al., 2011) (Allou and Zennir, 2018), fuzzy logics(Kodagoda et al., 2002), sliding mode control(Cristi et al., 1990), optimal state feedback controllers(Moriwaki, 2005), and model predictive control(Borrelli et al., 2005) for lateral and longitudinal control of the vehicle. Earliest autonomous vehicles such as Sandstrom used a simple geometric model for steering control (Urmson et al., 2006), whereas famous Stanley had their steering control model based on kinematic vehicle model (Thrun et al., 2006). Boss used model predictive control to perform vehicle control(Urmson et al., 2008).

We have developed our self-driving car, shown in Figure. 1. It is equipped with state-of-the-art sensors, including Lidar, GPS, IMU, camera, and radar. The architecture of our self-driving car consists of 4 layers: 1) sensor layer that perceives the data from the environment. 2) Perception layer, which consists of localization and detection. We have used data from the Lidar sensor to localize our self-driving car using NDT matching (Munir et al., 2019). The object detection is performed in image and Lidar data individually, and the results are fused and transformed into the world frame. 3) The planning layer takes information from the perception layer to determines the path followed by the self-driving car. It takes into account the geometry of the world and finds the safest path to follow while obeying the traffic rules and 4) The control layer receives the direction and speed information from planning and converts it into the control signal for car actuators, which enables it to drive autonomously.

In this work, we have proposed a vehicle dynamics model that plays an integral role in the execution of desired actions required by the autonomous car to follow the specified path. The planning module generates the velocity profile and trajectory that is needed to be followed. In order to ensure the velocity profile is properly followed, we have designed a customized PID controller for longitudinal control. For the lateral control, we have utilized both Pure Pursuit and Model Predictive Control based path follower and analyzed their behavior on the lateral dynamics model. The operation of longitudinal control is tested with two different speed ranges: low $(0-10km/h)$ and high $(10-30km/h)$.

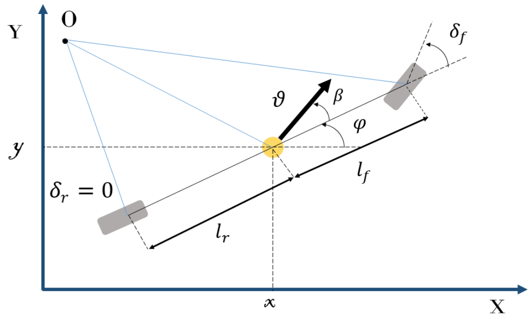

Figure 2: Kinematic Bicycle Model.

2 VEHICLE MODEL

Vehicle model provides the essential foundation for studying the characteristics of vehicle control, and therefore, a proper model of vehicle leads to robust and definite modeling of vehicle control(Limebeer and Massaro, 2018). In this work, we have investigated two types of vehicle models i) kinematic bicycle model and ii) dynamic bicycle model for our self-driving car. These models are necessary for vehicle analysis in order to model the controller.

2.1 Kinematic Bicycle Model

The kinematic bicycle model is widely used for the analysis of vehicle characteristics (Rajamani, 2011) (Zhang et al., 2018). Figure.2 shows the kinematic bicycle model. In this model, the front two wheels and as well as the back two wheels are lumped into a single wheel, respectively. The front lumped wheel is located at the center of the front axle, and similarly, the rear lumped wheel has center at the rear axle. With the assumption, that the front wheel can only be steered, the kinematic model is given by equation(1)-(5)

$$\dot{x} = v\cos(\psi+\beta)\ , \tag{1}$$

$$\dot{y} = v\sin(\psi+\beta)\ , \tag{2}$$

$$\dot{\psi} = \frac{v}{l_r}(\beta)\ , \tag{3}$$

$$\dot{v} = a\ , \tag{4}$$

$$\beta = \arctan(\frac{l_r}{l_f+l_r}+\tan(\delta_f)))\ , \tag{5}$$

where, x and y corresponds to the coordinates of the center of mass in the inertial frame (X,Y). v is the

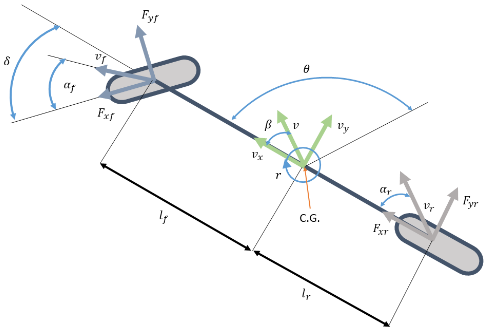

Figure 3: Dynamic Bicycle Model.

speed of the vehicle, and ψ denotes the heading of the vehicle. l_f and l_r represent the distance of lumped front wheel to the center of mass and vice versa. In this model, the control inputs are acceleration (a) and the steering angle (δ). For simplicity and, in general, practice the $\delta_r = 0$ because the only front wheel is considered to be steered.

This kinematic model is simple as compared to other models that include the forces (air resistance, the weight of the body) and friction. The kinematic model needs only two parameters (l_f and l_r) to be identified, and this makes it portable for both longitudinal and lateral control.

2.2 Dynamic Bicycle Model

The kinematic bicycle model only includes planar vehicle motions. The effect of forces acting on the body of the vehicle is overlooked in the simple kinematic model, which may impact the mild maneuvers. In order to address this problem, a 6 degree-of-freedom (DOF) dynamic vehicle model is formulated (Rajamani, 2011) (Zhou et al., 2019) . Figure. 3 shows the free body diagram of the vehicle. The governing equations for this model is shown from equation (6)-(10).

$$\ddot{x} = \dot{\psi}\dot{y} + a_x \, , \tag{6}$$

$$\ddot{y} = -\dot{\psi}\dot{x} + \frac{2}{m}(F_{c_f}\cos(\delta_f) + F_{c_r}) \, , \tag{7}$$

$$\ddot{\psi} = \frac{2}{I_z}(l_f F_{c_f} - l_r F_{c_r}) \, , \tag{8}$$

$$\dot{X} = \dot{x}\cos(\psi) - \dot{y}\sin(\psi) \, , \tag{9}$$

$$\dot{Y} = \dot{x}\sin(\psi) + \dot{y}\cos(\psi) \, , \tag{10}$$

where, the longitudinal and lateral speed is represented by $\dot{x}$ and $\dot{y}$, respectively, with respect to the body frame. The lateral forces on the rear and front wheel are denoted by F_{c_r} and F_{c_f}, respectively. The yaw rate, vehicle's mass, and yaw inertia are denoted by $\dot{\psi}$, m, and I_z, respectively. For the linear tire model, the F_{c_i} is defined by the equation (11).

$$F_{c_i} = -C_{\alpha_i}\alpha_i \, , \tag{11}$$

where, $i \in f, r$ and α_i is the slip angle given by equation (12)-(13) and C_{α_i} is the tire cornering stiffness.

$$\alpha_f = \arctan(\frac{v_y + l_f\dot{\psi}}{v_x}) - \delta \, , \tag{12}$$

$$\alpha_r = \arctan(\frac{v_y - l_r\dot{\psi}}{v_x}) \, , \tag{13}$$

3 LONGITUDINAL CONTROL

The longitudinal vehicle model is responsible for generating the velocity profile for the autonomous vehicle (Gao et al., 2017). In classical control theory, feedback controllers are used for compensating the error between the desired and observed measurements. Proportional-Integral-Derivative is one such kind of feedback controller that works on the propagation of error and minimizes it to achieve the desired response (Zakia et al., 2019) (Gambier, 2008). The control law for the PID control is given by equation (14).

$$u(t) = k_d\dot{e} + k_p e + k_i \int edt \, , \tag{14}$$

where, k_p, k_i and k_d are the proportional, integral and derivative gain for the PID controller and e is the error.

In our case, the velocity profile of the longitudinal vehicle control includes throttle, brake, and torque. For the vehicle to follow the velocity profile, a PID controller is used to minimize the error between current and target values of the throttle, brake, and torque. The current values are from the vehicle Controller-Area-Network (CAN) bus, and target values are from the planning module. This PID control is the customized longitudinal controller for our self-driving car because of the proprietary laws of KIA Company not sharing the CAN bus IDs, and the CAN bus IDs have been empirically found by implementing a can-sniffer algorithm.

The PID controller is designed in such a way that for each throttle, brake, and torque, two separate control parameters (values of K_p, K_i, and K_d) are used. The advantage of using this kind of framework gives the leverage of controlling the vehicle on high and low speed for throttle and also for the fast and slow application of torque to the steering wheel. Figure.4

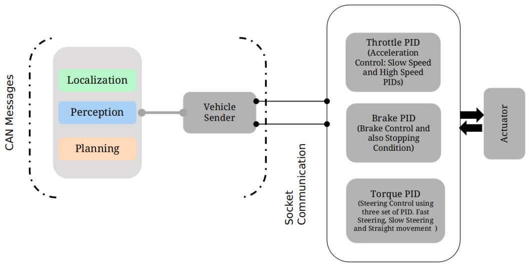
CAN Messages
Localization
Perception
Planning
Vehicle Sender
Socket Communication
Throttle PID (Acceleration Control: Slow Speed and High Speed PIDs)
Brake PID (Brake Control and also Stopping Condition)
Torque PID (Steering Control using three set of PID. Fast Steering, Slow Steering and Straight movement)
Actuator

Figure 4: The Longitudinal Control Is Composed of Throttle/brake and Torque Pids. The Controller Receives the Information from Vehicle Sender over Socket of Perception and Planning Modules.

show the framework for a PID controller that includes three components (i) Vehicle Sender (ii) Customized PID controller and (iii) Actuator. The vehicle sender serves as a communication bridge between the software stack and hardware stack and sends the planning commands over the socket to the customized controller.

4 LATERAL CONTROL

4.1 Pure Pursuit

Pure Pursuit is a path tracking algorithm that calculates the curvature from the current position to some goal position. The goal point is chosen such that it is always a constant distance ahead of vehicle current position (Coulter, 1992). In simpler terms, pure pursuit chase a moving goal points some distance ahead, called look-ahead distance. Figure.5 illustrate the basic principle of pure Pursuit. The current position of the vehicle is shown by (X,Y). The constant look-ahead distance denoted by L, goal point (X_L,Y_L) chased by the algorithm on the path. The radius R_t of the arc that joins the current position to the look-ahead point (X_L,Y_L). Based on two triangles, the following equation (15)-(17) are satisfied.

$$X_L^2+Y_L^2=L^2\ , \tag{15}$$

$$o_L^2+Y_L^2=R_t^2\ , \tag{16}$$

$$x_L+o=R_t\ . \tag{17}$$

The a in equation (17) is put into equation (16), resulting in:

$$(R_t-x_L)^2+Y_L^2=R_t^2\ , \tag{18}$$

$$R_t^2-2R_tx_L+X_L^2+Y_L^2=R_t^2\ , \tag{19}$$

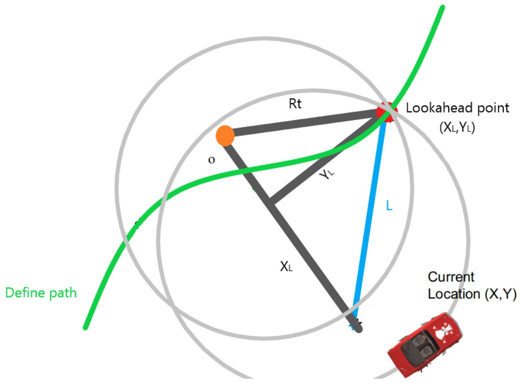

Figure 5: Basic Principle of Pure Pursuit Algorithm.

$$R_t=\frac{L^2}{2x_L}\ . \tag{20}$$

The R_t the arc radius determines the path followed by the vehicle.

4.2 Model Predictive Control

Model predictive control (MPC) incorporates the dynamics of the vehicle and controls the lateral motion of a vehicle while satisfying a set of constraints (Liu et al., 2017) (Sun et al., 2018). Model predictive control finds the optimal trajectory by solving an optimization problem at each time step and generates an actuator signal based on the finite horizon. The optimization formulation of MPC for lateral control using the kinematic and dynamic bicycle model after converting to the discrete model is given in equation (21)-(22).

$$\min_U \sum_{i=0}^{H_p}[(\mathbf{z}_i-\mathbf{z}_{ref,i})^T\mathbf{Q}(\mathbf{z}_i-\mathbf{z}_{ref,i})]+$$
$$\sum_{i=0}^{H_p-1}\ [(\mathbf{u}_i-\mathbf{u}_{i-1})^T\bar{R}(\mathbf{u}_i-\mathbf{u}_{i-1})+\mathbf{u}_i^TR\mathbf{u}_i]\ , \tag{21}$$

$s.t$

$$\mathbf{z}_0=\mathbf{z}(t),\mathbf{u}_{-1}=\mathbf{u}(t-t_s)\ ,$$

$$\mathbf{z}_{i+1}=f(\mathbf{z}_i,\mathbf{u}_i),i=0,...,H_p-1\ ,$$

$$\mathbf{u}_{min,i}\leqslant\mathbf{u}_i\leqslant\mathbf{u}_{max,i},\forall i\ ,$$

$$\dot{\mathbf{u}}_{min,i}\leqslant\frac{\mathbf{u}_i-\mathbf{u}_{i-1}}{t_d}\leqslant\dot{\mathbf{u}}_{max,i},\forall i/0\ ,$$

$$\dot{\mathbf{u}}_{min,i}\leqslant\frac{\mathbf{u}_i-\mathbf{u}_{i-1}}{t_s}\leqslant\dot{\mathbf{u}}_{max,i},i=0\ ,$$

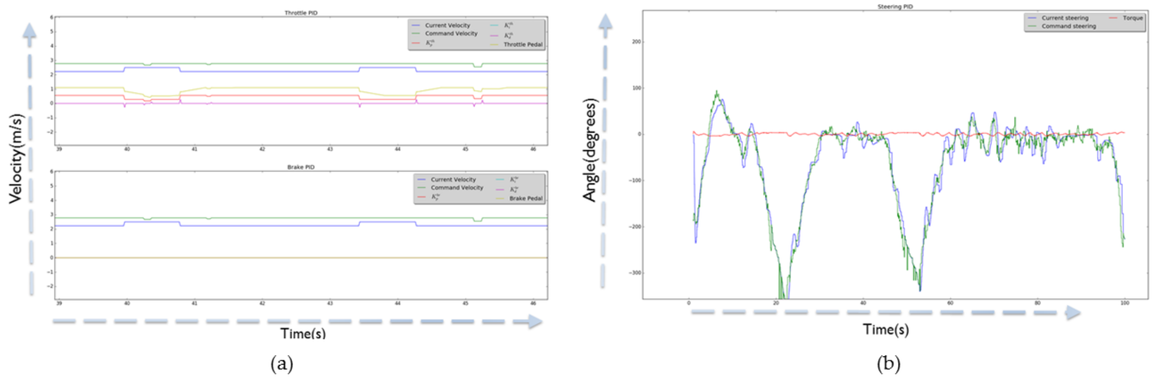

Figure 6: The PID Tuned Graphs for Throttle/brake and Torque. (a) the Command Velocity Is from the Planning and Current Velocity Is from the CAN Bus of Vehicle. The Throttle Pedal and PID Parameters (K_p,K_i and K_d) Are Also Shown. The Graph Also Shows the Variation of Each Term ($k_d\dot{e}$, k_pE and $k_i\int EDt$) of PID Controller with Respect to Current and Target Velocity. (B) Torque PID Tuned Graph Shows the Torque Value Applied to Vehicle after Parameters Are Tuned.

where $Q \in \mathbb{R}^{4x4}$, $R \in \mathbb{R}^{2x2}$, $\bar{R} \in \mathbb{R}^{2x2}$, H_p is the horizon prediction. The cost weights is represented by the diagonal matrices $\mathbf{Q}$, R, $\bar{R}$. The sampling time of the controller is t_s. The system dynamics after discretizing the vehicle kinematics model is given by $f(\mathbf{z}_i, \mathbf{u}_i)$ where $\mathbf{u}_{-1}$ is the input given to previous sampling step $\mathbf{u}(t-t_s)$. The constraints variables are represented for lower and upper bound are given by $\mathbf{u}_{min}$, $\bar{\mathbf{u}}_{max}$ and $\mathbf{u}_{max}$, $\bar{\mathbf{u}}_{max}$ respectively. The reference trajectory is given by $\mathbf{z}_{ref}$.

The MPC formulation to cater the vehicle dynamic model is given in equation (22).

$$\min_{U} \sum_{i=0}^{H_p} [(\mathbf{z}_i - \mathbf{z}_{ref,i})^T Q(\mathbf{z}_i - \mathbf{z}_{ref,i})] +$$

$$\sum_{i=0}^{H_p-1} [R(\triangle(F_{y_f}(k+i))^2 + \mathbf{W}\varepsilon_v] \,, \tag{22}$$

where, $\triangle \mathbf{F_{y_f}} = [\triangle F_{y_f}(k), \triangle F_{y_f}(k+1),..,\triangle F_{y_f}(k+H_{p-1})]$. ε_v is the non-negative slack variable. $\mathbf{Q}$, R and $\mathbf{W}$ are the weighting matrices.

5 EXPERIMENTATION AND RESULTS

In this section, we have experimented and evaluated the longitudinal and lateral control on our self-driving car.

5.1 Longitudinal Control

The vehicle longitudinal control is responsible to cater the throttle, brake, and torque (for the steering wheel) applied to the self-driving car. This is achieved by designing a PID controller. The PID controller is based on three parameters, given by equation (14), that are optimized for the robustness of the controller. These three parameters are proportional (K_p), integral (K_i) and derivative (K_d). The optimized tuning of these parameters is essential for the working of the controller. In our work, we have used two approaches for tuning the parameters of the PID i) Cohen-Coon method and ii) Genetic Algorithm.

Table 1: Quantitative Comparison between Cohen-Coon Method and Genetic Algorithm.

Controller Parameters	Throttle		Torque	
	Cohen-Coon Method	Genetic Algorithm	Cohen-Coon Method	Genetic Algorithm
K_p	0.085	0.003	0.0009	0.0005
K_i	0.0045	0.0001	0.0001	0.0002
K_d	0.01	0.09	0.0005	0.0008

In the Cohen-Coon method, first, the K_p parameter is tuned while the rest two parameters K_i and K_d are kept at zero. The other two parameters are tuned when the K_p parameter is optimized. Figure.6 shows the tuned PID graphs for throttle, brake, and torque.

The parameter's tuning using the Cohen-Coon method requires human supervision and tedious to do manually. In order to tune the parameters dynamically, we used the genetic algorithm for parameter tuning. The parameter tuning problem is formulated as an optimization problem with the focus on minimizing the error between current and target values for each throttle, brake, and torque. Table.1 shows the quantitative analysis of PID parameters tuned with the genetic algorithm and Cohen-Coon method. The PID parameter tuned using genetic algorithm approaches to the same values as obtained using the Cohen-coon method; hence it verifies the mathematical formulation of PID using the genetic algorithm, which provides dynamic tuning of PID parameters.

Table 2: Model Predictive Control Based Path Follower Design Parameters.

MPC parameters	Description	Value
QP solver type used for optimization	QP solver option	Unconstraint-fast
QPoases(solver) max iteration	maximum iteration number for convex optimiaztion with qpoases.	500
Vehicle Model type	vehicle model option. described below in detail.	Kinematics/Dynamic
Prediction horizon	total prediction step for MPC	70
Prediction sampling time	prediction period for one step [s]	0.1
Lateral weight error	Weight for lateral error in matrix Q	0.1
Heading weight error	Weight for heading error in matrix Q	0
Weight heading Error squared velocity coefficient	Lateral Heading Error * Velocity	5
Steering Weight Input	Steering weight error in matrix R (steer command - reference steer)	1
Weight Steering Input squared velocity coefficient	Steering error (steer command - reference steer) * velocity	0.25
Lateral Weight Jerk	Weight for lateral jerk (steer(i) - steer(i-1)) * velocity	0
Wheel base	Wheel base length for the vehicle model (meters)	2.95
Steering tau	Steering dynamics time constant (1d approximation) for vehicle model	0.3
Steering Limit	Steering angle limit (deg)	35
Steering Gear Ratio	Ratio between the turn of the steering wheel (in degree) to the turn of the wheel (in degree)	15

5.2 Lateral Control

For the lateral control of the self-driving car, we have used two path tracking controller i) pure pursuit and ii) MPC-based path follower. The robustness of these two controllers relies on the proper tuning of parameters based on the vehicle model. In the case of pure pursuit, the tuned parameters are shown in Table.3. As pure pursuit mainly depends on the look-ahead distance, we evaluated the performance of pure pursuit by changing the look-ahead distance. Figure.7 shows the result of the effect of look-ahead distance on the lateral control using pure pursuit. The closer look-ahead distance in pure pursuit leads to more noise and disturbance in the lateral control, whereas the greater look-ahead distance provides more deviation of the car from the specified ground-truth path. Similarly, the MPC parameters are optimized, as shown in Table.2.

In order to make a comparative analysis between the pure pursuit and MPC-based path follower, both the algorithms are applied to the vehicle at a speed of 30Km/h. Figure.8 shows the comparison result qualitatively. It can be seen that in the case of pure pursuit, the vehicle over-cuts the predefined (ground-truth) path at corner points, besides the MPC based path follower follows the ground-truth path more accurately. The quantitative analysis is done by finding the lateral error between both pure pursuit and MPC based path follower. Figure.9 shows the graph of lateral error between pure pursuit and MPC based path follower. The difference between pure pursuit and MPC can be significantly observed at the curved roads; the MPC does not overshoot and accurately follows the predefined (ground-truth) path. This ensures the safety of the car when making turns at narrow roads.

Table 3: Pure Pursuit Tuned Parameters for 30 Km/h Speed.

Pure Pursuit Parameters	Values
Look-ahead ratio	2
Minimum Look-ahead Distance	6

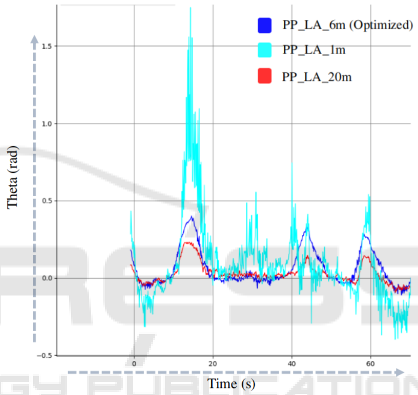

Figure 7: Effect of Look-Ahead Distance in Pure Pursuit. The Legends of the Graph Shows the Look-Ahead Distances, for Instance PP-LA-1m Is 1m Look-Ahead Distance in the Pure Pursuit. The 1m Look-Ahead Distance Is More Prone to Noise and Produce More Vibrations in the Lateral Model of Vehicle. Similarly the the 20m Look-Ahead Distance Deviates from Original Track and Overlook the Ground-Truth Waypoints. The Optimized Look-Ahead Distance Gives the Result with Minimal Error in Contrast to Other Look-Ahead Distance. Theta (Rad) Shows the Steering Angle for Lateral Control.

6 CONCLUSIONS

The control of the self-driving car plays a monumental role in the execution of decision commands to the

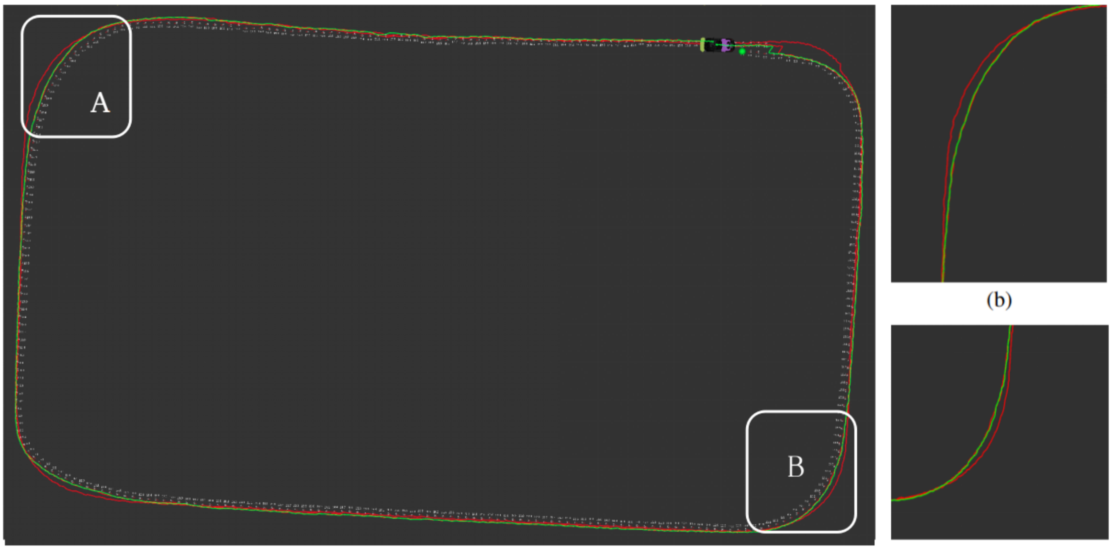

(a) (b) (c)

Figure 8: Qualitative Comparison between Pure Pursuit and Mpc Path Follower. The Red Color Line Shows the Pure Pursuit and the Green Color Corresponds to Mpc Path Follower. The Ground-Truth Path Is Shown by White Color. The Difference in Corners (a) and (B) Are Shown in (B) and (C) Respectively.

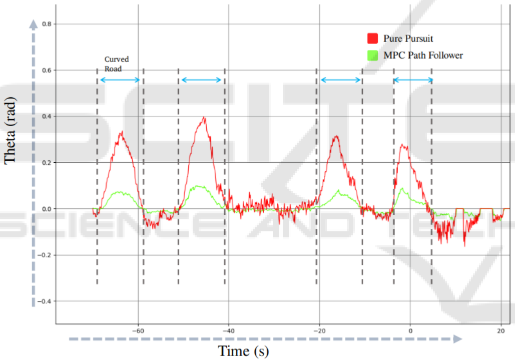

Figure 9: The Graphs Show the Difference between MPC and Pure Pursuit. The Difference between the Graphs Shows the Lateral Error. Theta (Rad) Shows the Steering Angle for Lateral Control in Case of Both MPC and Pure Pursuit.

vehicle. In this work, we have exploited the control of the self-driving car and implemented two control models i) longitudinal and ii) lateral control based on the kinematic and dynamic bicycle model. For the longitudinal control, a customized PID control is developed, and two approaches are discussed in tuning the parameters of this controller. Pure pursuit controller and model predictive control-based path follower are analyzed in the context of lateral control. The parameters of both controls are optimized in regard to our self-driving car.

ACKNOWLEDGMENT

This work is in part supported by GIST Research Institute (GRI) grant funded by the GIST in 2020.

REFERENCES

Apollo. http://apollo.auto/index.html.

SAE J3016. https://www.sae.org/news/2019/01/sae-updates-j3016-automated-driving-graphic.

Acosta, M., Kanarachos, S., and Fitzpatrick, M. E. (2017). A hybrid hierarchical rally driver model for autonomous vehicle agile maneuvering on loose surfaces. In *Proceedings of the 14th International Conference on Informatics in Control, Automation and Robotics - Volume 2: ICINCO,*, pages 216–225. INSTICC, SciTePress.

Allou, S. and Zennir, Y. (2018). A comparative study of pid-pso and fuzzy controller for path tracking control of autonomous ground vehicles. In *Proceedings of the 15th International Conference on Informatics in Control, Automation and Robotics - Volume 1: ICINCO,*, pages 306–314. INSTICC, SciTePress.

Borrelli, F., Falcone, P., Keviczky, T., Asgari, J., and Hrovat, D. (2005). Mpc-based approach to active steering for autonomous vehicle systems. *International Journal of Vehicle Autonomous Systems*, 3(2):265–291.

Coulter, R. C. (1992). Implementation of the pure pursuit path tracking algorithm. Technical report, Carnegie-Mellon UNIV Pittsburgh PA Robotics INST.

Cristi, R., Papoulias, F. A., and Healey, A. J. (1990). Adaptive sliding mode control of autonomous underwater vehicles in the dive plane. *IEEE journal of Oceanic Engineering*, 15(3):152–160.

Gambier, A. (2008). Mpc and pid control based on multi-objective optimization. In *2008 American Control Conference*, pages 4727–4732. IEEE.

Gao, H., Zhang, X., Liu, Y., and Li, D. (2017). Longitudinal control for mengshi autonomous vehicle via gauss cloud model. *Sustainability*, 9(12):2259.

Jiang, J. and Astolfi, A. (2018). Lateral control of an autonomous vehicle. *IEEE Transactions on Intelligent Vehicles*, 3(2):228–237.

Jun, N., Jibin, H., et al. (2018). Autonomous driving system design for formula student driverless racecar. In *2018 IEEE Intelligent Vehicles Symposium (IV)*, pages 1–6. IEEE.

Kodagoda, K., Wijesoma, W. S., and Teoh, E. K. (2002). Fuzzy speed and steering control of an agv. *IEEE Transactions on control systems technology*, 10(1):112–120.

Lee, M., Yun, J., Pyka, A., Won, D., Kodama, F., Schiuma, G., Park, H., Jeon, J., Park, K., Jung, K., et al. (2018). How to respond to the fourth industrial revolution, or the second information technology revolution? dynamic new combinations between technology, market, and society through open innovation. *Journal of Open Innovation: Technology, Market, and Complexity*, 4(3):21.

Limebeer, D. J. and Massaro, M. (2018). *Dynamics and optimal control of road vehicles*. Oxford University Press.

Liu, C., Lee, S., Varnhagen, S., and Tseng, H. E. (2017). Path planning for autonomous vehicles using model predictive control. In *2017 IEEE Intelligent Vehicles Symposium (IV)*, pages 174–179. IEEE.

Moriwaki, K. (2005). Autonomous steering control for electric vehicles using nonlinear state feedback h control. *Nonlinear Analysis: Theory, Methods & Applications*, 63(5-7):e2257–e2268.

Munir, F., Azam, S., Hussain, I., Sheri, A. M., and Jeon, M. (2018). Autonomous Vehicle: The Architecture Aspect of Self Driving Car.

Munir, F., Azam, S., Sheri, A., Ko, Y., and Jeon, M. (2019). Where Am I: Localization and 3d Maps for Autonomous Vehicles. In *5th International Conference on Vehicle Technology and Intelligent Transport Systems (VEHITS)*, pages 452–457.

Pérez, J., Milanés, V., and Onieva, E. (2011). Cascade architecture for lateral control in autonomous vehicles. *IEEE Transactions on Intelligent Transportation Systems*, 12(1):73–82.

Rajamani, R. (2011). Vehicle dynamics and control, ser. *Mechanical Engineering Series. Springer*, page 26.

Rupp, A. and Stolz, M. (2017). *Survey on Control Schemes for Automated Driving on Highways*, pages 43–69. Springer International Publishing, Cham.

Sun, C., Zhang, X., Xi, L., and Tian, Y. (2018). Design of a path-tracking steering controller for autonomous vehicles. *Energies*, 11(6):1451.

Thomanek, F. and Dickmanns, E. D. (1995). Autonomous road vehicle guidance in normal traffic. In *Asian Conference on Computer Vision*, pages 499–507. Springer.

Thrun, S., Montemerlo, M., Dahlkamp, H., Stavens, D., Aron, A., Diebel, J., Fong, P., Gale, J., Halpenny, M., Hoffmann, G., et al. (2006). Stanley: The robot that won the darpa grand challenge. *Journal of field Robotics*, 23(9):661–692.

Urmson, C., Anhalt, J., Bagnell, D., Baker, C., Bittner, R., Clark, M., Dolan, J., Duggins, D., Galatali, T., Geyer, C., et al. (2008). Autonomous driving in urban environments: Boss and the urban challenge. *Journal of Field Robotics*, 25(8):425–466.

Urmson, C., Ragusa, C., Ray, D., Anhalt, J., Bartz, D., Galatali, T., Gutierrez, A., Johnston, J., Harbaugh, S., “Yu” Kato, H., et al. (2006). A robust approach to high-speed navigation for unrehearsed desert terrain. *Journal of Field Robotics*, 23(8):467–508.

Zakia, U., Moallem, M., and Menon, C. (2019). Pid-smc controller for a 2-dof planar robot. In *2019 International Conference on Electrical, Computer and Communication Engineering (ECCE)*, pages 1–5. IEEE.

Zhang, R., Abraham, A., Dasgupta, S., and Dauwels, J. (2018). Constrained model predictive control using kinematic model of vehicle platooning in vissim simulator. In *2018 15th International Conference on Control, Automation, Robotics and Vision (ICARCV)*, pages 721–726. IEEE.

Zhou, S., Liu, Z., Suo, C., Wang, H., Zhao, H., and Liu, Y.-H. (2019). Vision-based dynamic control of car-like mobile robots. In *2019 International Conference on Robotics and Automation (ICRA)*, pages 6631–6636. IEEE.

Ziegler, J., Bender, P., Schreiber, M., Lategahn, H., Strauss, T., Stiller, C., Dang, T., Franke, U., Appenrodt, N., Keller, C. G., et al. (2014). Making bertha drive—an autonomous journey on a historic route. *IEEE Intelligent transportation systems magazine*, 6(2):8–20.